Asociación Argentina
de Mecánica Computacional

Mecánica Computacional Vol XXIX, págs. 3601-3611 (artículo completo)
Eduardo Dvorkin, Marcela Goldschmit, Mario Storti (Eds.)
Buenos Aires, Argentina, 15-18 Noviembre 2010

NUMERICAL SIMULATIONS OF NAVIER STOKES FOR TRANSIENT FLOWS IN 2D

Diomar Cesar Lobão

Departamento de Ciências Exatas, Universidade Federal Fluminense,Av. dos Trabalhadores 420, Vila Santa Cecilia, CEP 27255-125, Volta Redonda, RJ, Brasil, lobaodiomarcesar@yahoo.ca

Keywords: Viscous flow, Shockwave, Transient high speed flows.

Abstract. The present work describes the numerical simulations of transient flows in two dimensional geometries with shock waves involving multiple shocks and reflections of shockwaves, and their interactions. The numerical formulations solve the fully compressible Navier Stokes equations set using explicit Mac Cormack method. The numerical simulated results are compared against well validated solutions based on different implementations and methods. In this work the primary intention is investigate the no-slip boundary condition behavior. The numerical simulated results were compared with high resolution TVD numerical results and good agreements were obtained. These numerical simulations have also revealed that the NS formulation is very sensible to the mesh used and its solution becomes unstable as a function of mesh density and quality.

1 INTRODUCTION

In order to simulate the compressible Navier Stokes governing equations, a 2D solver has been developed and implemented for transient flows in various Mach number and also different geometries. The Navier Stokes governing equations are solved by an explicit second order accurate finite volume spatial discretization as discussed by MacCormack (1969), MacCormack and Baldwin (1975), Jameson et al. (1981), Furst and Kozel (2001) and Dick (1990). The solver is designed in order to simulate the Euler equations as well as the Navier Stokes. In the present work, the effective converged solution is analyzed under the application of the no-slip boundary condition as well as the influence of the mesh used in the simulations. The simulations has shown that once the mesh is calibrated the solution converge to the expected steady state.

2 GOVERNING EQUATIONS

The two-dimensional continuity, x and y momentum and energy equations describing the non-turbulent flow of a compressible fluid expressed in strong conservation form in the cartesian coordinate system are written as following

$$\frac{\partial q}{\partial t}+\frac{\partial F}{\partial x}+\frac{\partial G}{\partial y}=0 \tag{1}$$

Where q represents the conserved variables. F and G are the overall fluxes in (x, y) directions respectively and are given by:

$$F = F_c - F_v, \tag{2}$$

$$G = G_c - G_v, \tag{3}$$

and

$$q=\begin{pmatrix}\rho\\ \rho u\\ \rho v\\ E\end{pmatrix},\qquad F_c=\begin{pmatrix}\rho u\\ \rho u^2+P\\ \rho uv\\ (E+p)u\end{pmatrix},\qquad G_c=\begin{pmatrix}\rho v\\ \rho uv\\ \rho v^2+P\\ (E+p)v\end{pmatrix},$$

$$F_v=\begin{pmatrix}0\\ \frac{4}{3}\mu\frac{\partial u}{\partial x}-\frac{2}{3}\mu\frac{\partial v}{\partial y}\\ \mu\frac{\partial u}{\partial y}+\mu\frac{\partial v}{\partial x}\\ k\frac{\partial T}{\partial x}+\frac{4}{3}\mu u\frac{\partial u}{\partial x}-\frac{2}{3}\mu u\frac{\partial v}{\partial y}+\mu v\frac{\partial u}{\partial y}+\mu v\frac{\partial v}{\partial x}\end{pmatrix},\qquad G_v=\begin{pmatrix}0\\ \mu\frac{\partial u}{\partial y}+\mu\frac{\partial v}{\partial x}\\ \frac{4}{3}\mu\frac{\partial v}{\partial y}-\frac{2}{3}\mu\frac{\partial u}{\partial x}\\ k\frac{\partial T}{\partial y}+\frac{4}{3}\mu v\frac{\partial v}{\partial y}-\frac{2}{3}\mu v\frac{\partial u}{\partial x}+\mu u\frac{\partial u}{\partial y}+\mu u\frac{\partial v}{\partial x}\end{pmatrix},$$

Where ρ is the density, (u, v) the velocity vector, E the total energy per unit volume $E = e + (u^2 + v^2)/2$, $e = c_v T$ the internal energy, μ the viscosity coefficient, and k is the heat conductivity, p is the pressure, γ is the heat adiabatic coefficient, and the components of the stress tensor τ are given in F_v and G_v. The 2D Euler equations are obtained from the Navier Stokes equations by setting μ = k = 0.

2.1 Boundary Conditions

The flow simulation requires defining the boundary conditions on the solid walls. Mainly two types of closed boundary conditions can be imposed on the wall in the simulation: no-slip boundary (velocity vector equal to zero) and free-slip (slip) boundary implying that only normal to the wall direction component of velocity reduced to zero guaranteeing the velocity tangency condition. In the second case, the tangential component can be different from zero. However, its derivative in the direction normal to the wall equals zero. For the Euler equations is specified only the normal component of the velocity (for example, to be zero at a stationary solid wall). The solution of the Euler equation can lead to a slip velocity at the wall. However, for the NS equations, which are of one order higher, it is need to specify the tangential component also. Note that there is no need for it to be zero to solve the equations but its precise description is required. More detailed discussion is found in Arakeri and Shankar (2000). The influence of the boundary condition type on numerical results of 2D channel flow computation is investigated in the paper. The computations obtained using both boundary condition types are compared to numerical simulation. In order to cover a large variety of possible flow situations it is assumed four types of boundary conditions for the equations set given by eq(1) as follow Furst and Kozel (2001):

a) Inlet: At the inlet it is prescribed the direction of the velocity. The stagnation density ρ0 and the stagnation pressure p0. Extrapolation of the static pressure p from inside is carried out and computes the other required quantities using the following relations between the stagnation and the static quantities: $p_0 = p(1+(\gamma-1)/2M^2)^{\gamma/(\gamma-1)}$ and $\rho_0 = \rho(1+(\gamma-1)/2M^2)^{1/(\gamma-1)}$, where M is the local Mach number defined by $M = \sqrt{u^2+v^2}/a$ where the local speed of sound is $a = \sqrt{\gamma p/\rho}$. For the Navier Stokes equations it is assumed $\partial T/\partial \vec{n} = 0$ and q_∞ given.

b) Outlet: At the outlet it is prescribed the value of the static pressure *p* and extrapolates the values of the density ρ and of the velocity vector from the flow field. For the viscous flows we assume again $\partial T/\partial \vec{n} = 0$.

c) Solid wall: It is prescribed the tangential condition $\vec{V}.\vec{n} = 0$ for the inviscid flow or no-slip boundary condition $\vec{V} = 0$ for the viscous flows. It is also assumed the adiabatic walls (i.e. $\partial T/\partial \vec{n} = 0$ where *T* is the temperature).

d) Periodicity: It is prescribed the periodical condition for all components of the vector of unknowns *q*. This boundary condition is implemented as cycled as: $w_{i=1} = w_{i=n-1}, w_{i=2} = w_{i=n}$, where *w* is unknown *q*. This is a classical procedure for channel flow.

The discretization is carried out based on a cell-vertex formulation, and the flow variables are stored at cell vertices. Studies elsewhere have been done as given by Dick (1990), Martinelli (1987), Swanson and Radespiel (1991) showing that cell-vertex formulation has some advantages over the cell-centered. As for example, having a uniform mesh, there is no difference between the cell-centered and cell-vertex formulation. The cell-vertex scheme does not require extrapolation to the solid boundary to obtain the wall static pressure since it is already there calculated.

Schemes based on central-difference generate oscillations near a discontinuity. However, such schemes can be stabilized by introducing a small amount of artificial viscosity. The

artificial viscosity used in the present work, is that proposed by Jameson et al. (1981) modified to fit the cell-vertex formulation. This is a blend of second and fourth-order terms with a pressure switch to detect changes in pressure gradient. The time integration is done by means of an explicit two-stage time stepping scheme, MacCormack (1969). Explicit methods have been seem with caution because they have a limitation on the maximum size of the time step which can used without the appearance of random disturbances increasing boundlessly. As consequence the numerical simulation must often proceed slowly. However, now days, the speed of a desktop computer might offset this limitation on the time step making an explicit scheme a practical scheme.

3 COORDENATE TRANSFORMATION OF THE GOVERNING EQUATION

Following the coordinate transformation $(x,y) \rightarrow (\xi(x,y),\eta(x,y))$ Anderson et al. (1984) is possible to rewrite the set of equations as given by eq (1) as follow:

$$\frac{\partial q^{"}}{\partial t} + \frac{\partial F^{"}}{\partial \xi} + \frac{\partial G^{"}}{\partial \eta} = 0 \tag{4}$$

$$\begin{cases} q^{"} = Jq, \quad J = x_{\xi} y_{\eta} - x_{\eta} y_{\xi} \\ F^{"} = y_{\eta} F - x_{\eta} G = J(\xi_x F + \xi_y G) - F^{"v}_{i,j} \\ G^{"} = -y_{\xi} F + x_{\xi} G = J(\eta_x F + \eta_y G) - G^{"v}_{i,j} \end{cases} \tag{5}$$

The MacCormack (1969) method written for this transformed domain is:

$$\begin{cases} 1^{\circ}\ step \ - \ \text{Predictor} \\ q^{*}_{i,j} = q^{n}_{i,j} - \dfrac{\Delta t}{J_{i,j}} \left[(F^{"n}_{i+1,j} - F^{"n}_{i,j}) + (G^{"n}_{i,j+1} - G^{"n}_{i,j}) \right] \\ 2^{\circ}\ step \ - \ \text{Corrector} \\ q^{n+1}_{i,j} = \dfrac{1}{2} \left\{ (q^{n}_{i,j} + q^{*}_{i,j}) - \dfrac{\Delta t}{J_{i,j}} [(F^{"*}_{i,j} - F^{"*}_{i-1,j}) + (G^{"*}_{i,j} - G^{"*}_{i,j-1})] \right\} \end{cases} \tag{6}$$

The artificial diffusion terms $F^{"v}_{i,j}, G^{"v}_{i,j}$ added Jameson et al. (1981), Furst and Kozel (2001) have the same construction for each of the four dependent variables. For the density variable can be established by:

$$F^{"v}_{i,j} = 0.5(d_{i+1,j} - d_{i-1,j}); G^{"v}_{i,j} = 0.5(d_{i,j+1} - d_{i,j-1}) \tag{7}$$

$$d_{i+1,j} = \frac{1}{J_{i+1,j}} \left\{ \varepsilon^{(2)}_{i+1,j} (\rho_{i+1,j} - \rho_{i,j}) - \varepsilon^{(4)}_{i+1,j} \Phi_{i+1,j} \right\} \tag{8}$$

$$\Phi_{i+1,j} = \rho_{i+2,j} - 3\rho_{i+1,j} + 3\rho_{i,j} - \rho_{i-1,j} \tag{9}$$

$$\nu_{i,j} = \frac{\left| p_{i+1,j} - 2p_{i,j} + p_{i+1,j} \right|}{\left| p_{i+1,j} \right| + 2\left| p_{i,j} \right| + \left| p_{i-1,j} \right|} \tag{10}$$

Then

$$\begin{cases} \varepsilon^{(2)}_{i+1,j} = k^{(2)} \nu_{i,j} (|u''| + c)_{i+1,j} \\ \varepsilon^{(4)}_{i+1,j} = \max(0, (k^{(4)} - \varepsilon^{(2)}_{i+1,j}))(|u''| + c)_{i+1,j} \end{cases} \tag{11}$$

Where typical values of the constants $k^{(2)}$ and $k^{(4)}$ are

$k^{(2)} = \frac{1}{4}; \quad k^{(4)} = \frac{1}{256}$

The dissipation terms of the remaining components are obtained by substituting $\rho u, \rho v$ and E for ρ in the eq (8) and eq (9). In depth studies Jameson et al. (1981) reveled that in smooth regions of the flow field, the MacCormack method with dissipation is not sufficiently dissipative unless the fourth differences are included. Consequently the calculations will generally not converge to a completely steady state solution. Instead, after they have reached an almost steady state, oscillations of very low amplitude continue indefinitely being observed in the residual history graphic. The cause of this seems to be induced by pressure waves reflections from the boundaries of the computational domain. Near shock waves it has been found that the fourth differences tend to induce overshoots, and therefore they are switched off by subtracting $\varepsilon^{(2)}$ from $\varepsilon^{(4)}$ in eq (11). In the present Euler NS solver this has been verified.

4 SOLVER VALIDADTION

In order to ensure the validity of the solver, seeks for its ability to capture shocks, contact discontinuity and shocks interactions at same time being able to produce the correct pressure, density and speed profiles for the steady state. The approach used is the validation of the Euler solver against a numerical solution from a well established code capable of dealing strong shock waves based on the TVD scheme discussed by Lobão (1992). The compared solution is done using a benchmark case. The test case chosen is the transonic flow through the two-dimensional test channel with a bump of 4.2% of thickness, i.e. the so-called Ron-Ho-Ni channel. This is a well-known test case and it was solved by many researchers Rizzi and Vivand (1981). The grid size is 99x41, *M*=0.85, *p*=1.01e5Pascal, *T*=273K, *R*=287.05Nm/kgK, μ=1.7153e-5kg/s.m, k=3.4306e-6cal/cm.s.K and the *CFL*=0.4 has been used for both simulation, Euler and NS. In fig.1 is shown the grid used for this simulation. Notice the stretching Anderson et al. (1984) used close to both solid walls in the channel.

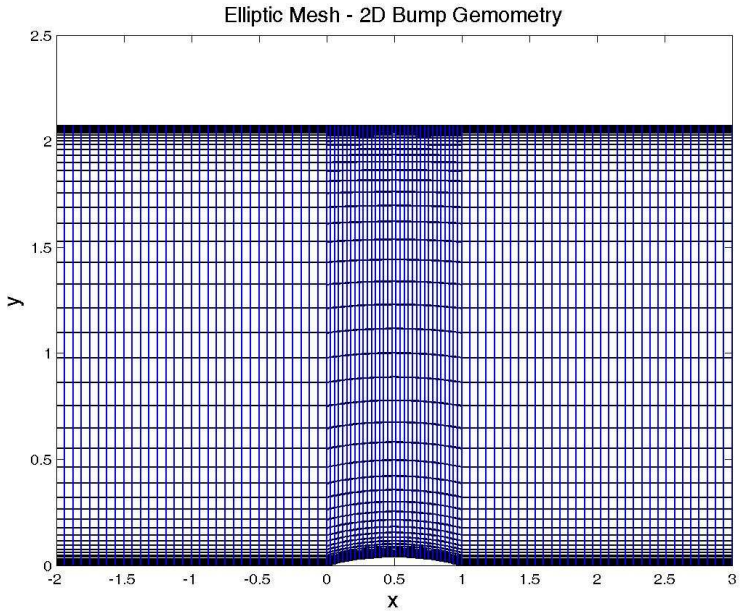

Fig. 1 Grid with double stretching function

In the fig.2 is shown the Cp value comparison on the lower wall for Euler, NS and TVD formulation. The shock is captured in the right position as the discontinuity jump through at most on three cells.

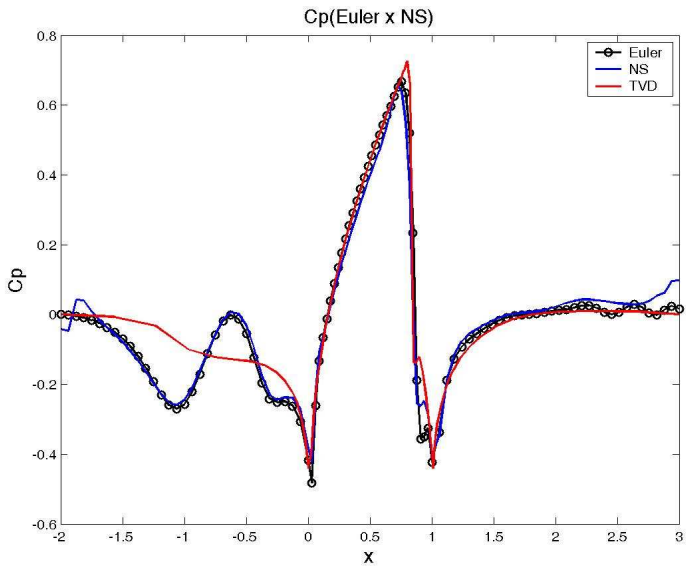

Fig. 2 Cp on the lower wall

The Mac Cormack method yields before the bump some oscillation in the Cp curve not present for the TVD scheme. Other results have shown that for less dense grids the NS solver won't converge. The next simulation is a double ramp channel with 10.1012º of elevation. The grid size of 120x40 and M=1.5. This geometry at this Mach number will reveal interesting flow structures as shock and it reflection on the upper solid wall. In fig. 3 is shown the mesh used. The fig. 4 shows the pressure field for NS simulation. As the mesh is highly

dense for this domain no stretching was considered.

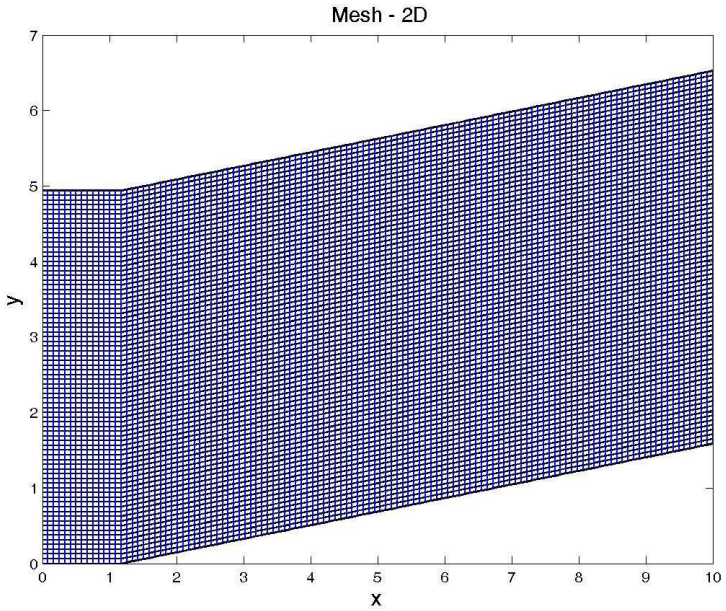

Fig. 3 Ramp mesh size 120x40

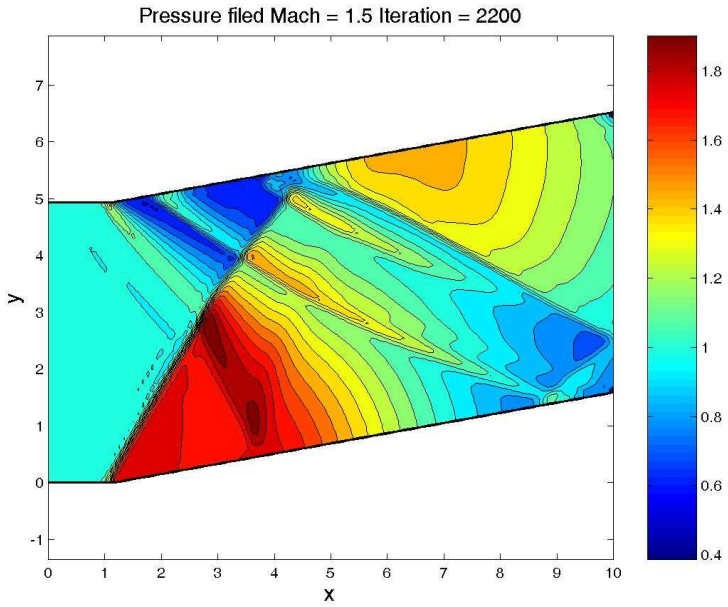

Fig. 4 Pressure filed for NS simulation

The next figure shows the Cp value from the lower surface precisely locating the shock at the ramp corner.

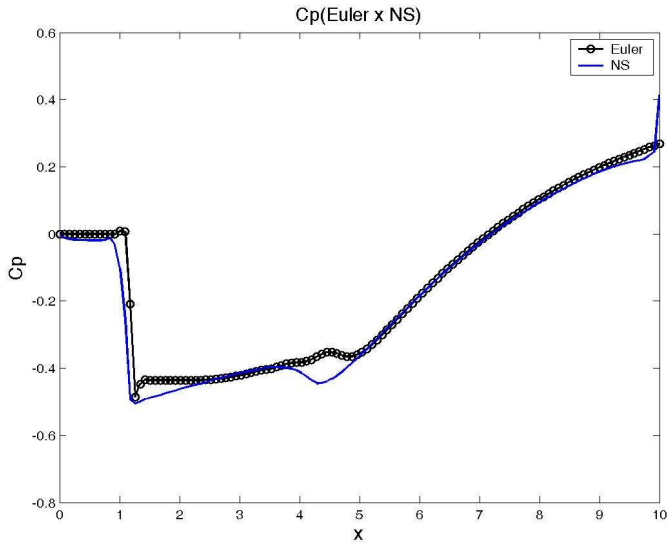

Fig. 5 Cp on the lower wall for Euler and NS

The next simulation will test the solver ability to capture a detached bow shock as well as the shock reflection from the main shock. The Mach number M=1.5 and the mesh size is 120x80 with double stretching near the walls and is shown in the fig. 6.

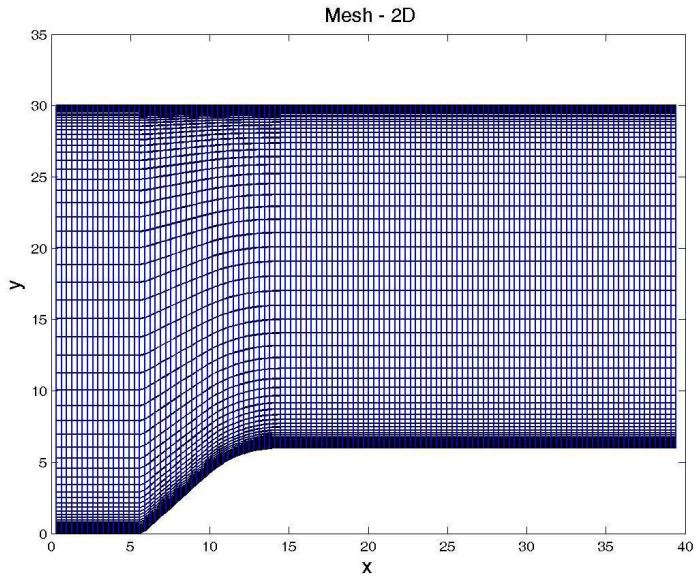

Fig. 6 Mesh with double stretching for NS

The fig. 7 shows the Mach number field for this simulation where is possible to observe the complex flow field before the ramp showing subsonic, transonic and supersonic regions. O the upper wall the incident shock wave reflects towards the lower wall.

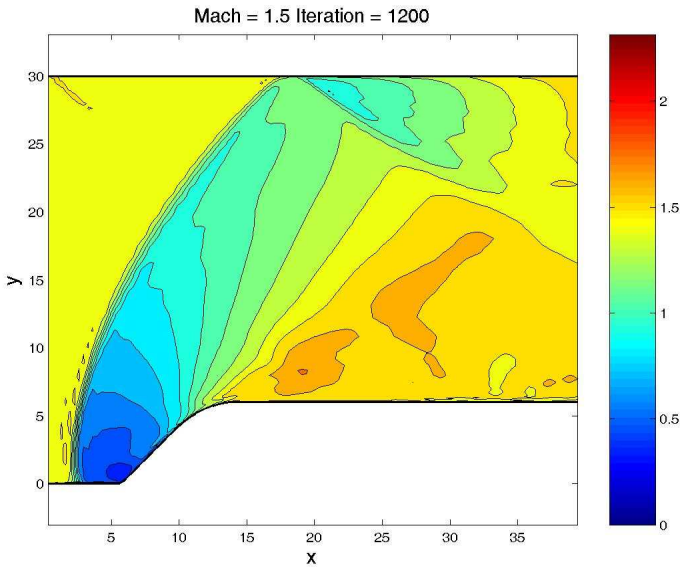

Fig. 7 Mach number flow field

The fig. 8 shows the pressure field where the shock reflection from the upper wall is better seen.

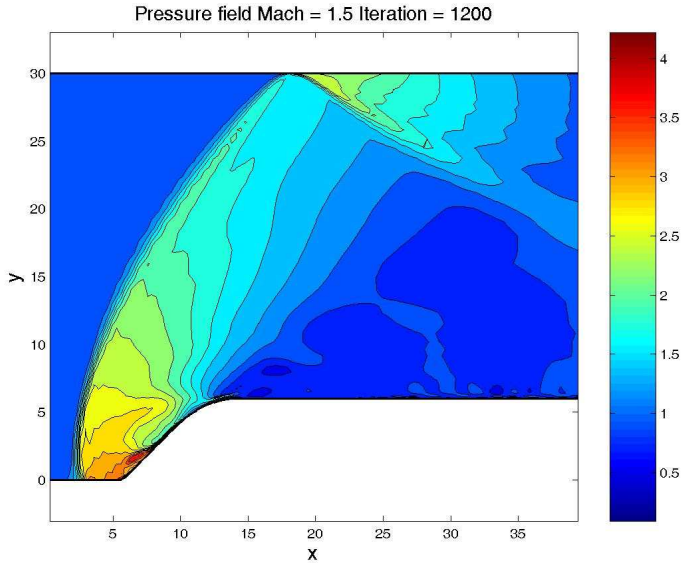

Fig. 8 Pressure filed for NS solution

Trying the NS solution for M=2.5 in the same mesh wasn't possible reach convergence in two situations: with and without stretching. However, that simulation for Euler the situation turned out to be successful. A more complex structure appears when M=2.5 is simulated for Euler solver. The development of a "Y" shock structure starts as the steady state is reached in 4200 iterations. The pressure flow field is shown in the fig. 9 as follow below.

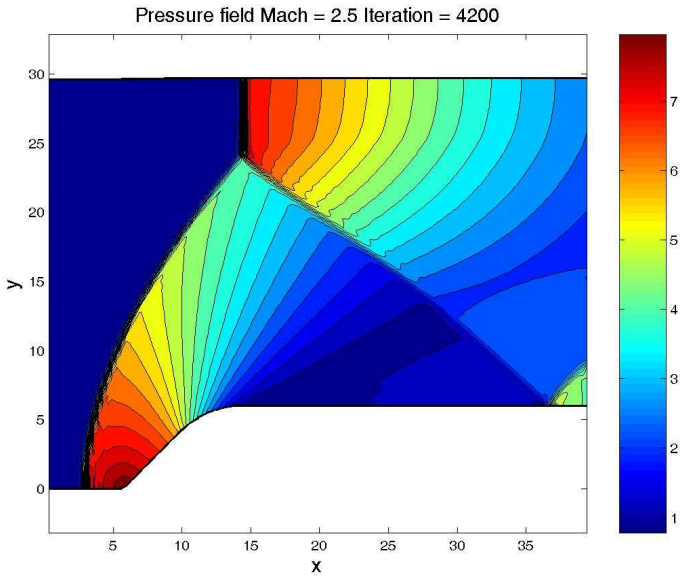

Fig. 9 Pressure field for M=2.5 showing the “Y” shock

5 ACKNOWLEDGEMENTS

I gratefully acknowledge Universidade Federal Fluminese and Pensa Rio Project for helpful financial support during this work.

6 CONCLUSIONS

The paper described the use of the Navier Stokes solver developed, implemented, and tested for simulation of flow in different velocity regimes. The solver has been applied to several case situations related to Mach number and geometries. The agreement with the analyzed solution is very good for same cases which proved the validity of the basic numerical scheme developed. However, it is shown that the NS solver introduce too much dissipation in other situations causing drastic failure of the solver. In general, the no-slip boundary condition implemented requiring stretching close the wall proved to be the correct one to those successful cases as discussed before.

REFERENCES

Mac Cormack, R.W., ‘The Effect of Viscosity in Hypervelocity Impact Cratering’, *AIAAPaper 1969-354*, Cincinnati, 1969.

Jameson, A., Schmidt, W. and Turkel, E., 'Numerical Solutions of the Euler Equations by Finite Volume Methods using Runge-Kutta Time Stepping Schemes' AIAA Paper n. 81-1259, 1981.

Furst, J., Kozel, K.,’Numerical Solution of Inviscid and Viscous Flows Using Modern Schemes and Quadrilateral or Triangular Mesh’ Mathematica Bohemica, n. 2, 379-393,Vol. 126, 2001.

Dick, E., ‘Introduction to Finite Volume Techniques’, V.K.I Lecture Series. 1990.

Lobão, D.C., 'High Resolution Schemes Applied to The Euler Equations', Ph.D. Theses, at University of Bristol, UK, 1992.
Rizzi, A. and Vivand, H., 'Numerical Methods for The Computation of Inviscid Transonic Flows With Shock Waves'. Notes on Numerical Fluid Mechanics. Vol.3, A GAMM Workshop, Vieweg and Sohn, 1981.
Martinelli, L., 'Calculations of Viscous Flows with a Multigrid Method', PhD Thesis, MAE Department, Princeton University, 1987.
Swanson, R.C. and Radespiel, R., 'Cell Centred and Cell Vertex Multigrid Schemes for the Navier Stokes Equations.'AIAA Journal, 1991.
R. W. Mac Cormack, B. S. Baldwin, 'A numerical method for solving the Navier-Stokes equations with application to shock-boundary layer interactions', AIAA Paper, 72-154, 1975.
Arakeri, J.H. and Shankar, P.N., 'Ludwig Prandtl and Boundary Layers in Fluid Flow', *Resonance*, Vol.5, No.12, pp. 48 – 63, 2000.
Anderson, D.A., Tannehill, J.C., Pletcher, R.H., 'Computational Fluid Mechanics and Heat Transfer', ISBN: 156032046X, 1984.